Unsteady Flow Analysis of Silicon Dioxide-Water and Silicon Dioxide-Kerosene Nanofluids Between Two Parallel Plates – Analytical Analysis

[1]Tapas Datta,
Department of Mathematics, A.K.P.C. Mahavidyalaya, Subhasnagar, Bengai, Hooghly, West Bengal, India.
Ph.D scholar, Dr. A P J Abdul Kalam University, Indore, Madhya Pradesh - 452016
Email: tapasdatta9999@gmail.com

[2]Dr. Annapurna Ramakrishna Sinde,
Department of Mathematics, Dr. A P J Abdul Kalam University, Indore, Madhya Pradesh - 452016
E-mail: jayabhandari15@gmail.com

[3] Dr. Md Tausif Sk,
Department of Mathematics, Acharya B N Seal College, Cooch Behar – 736101, West Bengal, India
Email: tausifdropbox@gmail.com

Article Info
Page Number: 13293 – 13298
Publication Issue:
Vol 71 No. 4 (2022)

Abstract: The current article researches the pressing progression of two sort of nanofluids like Silicon Dioxide-water and Silicon Dioxide-kerosene between two equal plates in presence of attractive field. The administering non-straight incomplete differential conditions are changed into common differential conditions by applying reasonable likeness change and afterward tackled mathematically utilizing RK-4 strategy with shooting procedure and systematically utilizing differential change technique (DTM). The impact of emerging applicable boundaries on stream attributes have been examined through diagrams and tables. A relative report has been considered between existing outcomes and present work and being as one is found.

Article History
Article Received: 25 October 2022
Revised: 30 November 2022
Accepted: 15 December 2022

Keywords: Squeezing flow; Nanofluid; Magnetic field; Differential transformation method.

INTRODUCTION:

The pressing progression of Newtonian and non-Newtonian liquids keep on animating huge interest by the specialists attributable to expanding application in various fields of designing, innovation, for example, polymer handling, transient stacking of mechanical parts, pressure, the crushed film in power transmission, moving cylinders, chocolate filler and so on. Such streams are performed between two moving equal plates. Traditional work in this area was first announced by Stefan [1] considering the pressing stream utilizing oil approach in 1874. After that Reynolds [2] considered the issues for elliptic plates in 1886. Archibald [3] examined the just barely getting move through rectangular plates in 1956. Bit by bit step by step extensive endeavors have been committed by the specialists to benefit the pressing stream simpler and

solid. Rashidi et al. [4] examined the two layered Axisymmetric pressing stream between equal plates. Impacts of attractive field in the crushing stream between limitless equal plates was accounted for by Siddiqui et al. [5]. Hamdan and Aristocrat [6] researched the crushing progression of dusty liquid between equal plates and talked about the pressing consequences for the speed profiles. Domairry and Aziz [7] conveyed the rough logical answer for the crushing progression of gooey liquid between equal circles with pull or blowing. Hayat et al. [8] expanded crafted by Domairry and Aziz [7] to examine the just barely getting stream of non-Newtonian liquids by requiring 2nd grade liquids.

As of late the investigation of intensity move qualities of a thick liquid in a pressing stream has acquired impressive consideration attributable to their applications in many parts of science and designing. The just barely getting move through a permeable surface has been tended to by Mahmood et al. [9]. Examination uncovers that greatness of neighborhood Nusselt number increments with Prandtl number. The outcomes are happy with Mustafa et al. [10]. Heat move qualities in a crushing stream between equal circles has been concentrated by Duwairi et al. [11]. Khaled and Vafai [12] dissected the hydromagnetic consequences for stream and intensity move over an even surface set in a remotely crushed free stream. They found that Nusselt number and wall shear pressure are both expanding elements of the attractive boundary. Logical examination of the temperamental crushing progression of gooey Jeffery liquid between equal plates was performed by Qayyum et al. [13] and examined the porosity and crushing impacts on the speed profiles.

The advanced age is appropriately called the period of science. Whenever we cast our eyes, we see that continuous cutting-edge innovation requires further improvement of intensity move according to energy saving perspective. Since the regular intensity move liquids, for example, water, kerosene, ethylene glycol have low warm conductivity, consequently current science gave favoring as nanofluid in which nano-sized particles are added to the base liquid to build the intensity move abilities of the base liquid. It ought to be seen that there have been distributed a few late papers [14-18] on the numerical and mathematical displaying of convective intensity move system in nanofluids. Mandy [19] examined blended convection stream and intensity move of nanofluids because of an insecure extending sheet. These models enjoy an upper hand over trial concentrates because of many variables that impact nanofluid properties. As of late, nanofluid stream and intensity move qualities under various stream setup was talked about by Hatami et al. [20, 21]. Logical examination of shaky crushing nanofluid stream has been talked about by Pourmehran et al. [22]. They showed that most noteworthy worth of Nusselt number can be acquired by choosing silver as nanoparticle.

Presently a day's cutting-edge science, designing fields are honored with such countless mathematical and scientific techniques to get exact rough arrangements from non-straight conditions. The strategies are like variety of boundary strategy (VPM) [23, 24], differential change technique (DTM) [25, 26], Adomian disintegration strategy (ADM) [27, 28], homotopy investigation technique (HAM) [29] and so on. In this article we have applied somewhat an original scientific strategy, say differential change technique (DTM) which can be said as an adjusted variant of Taylor series technique. It is the technique where we decide the coefficient of Taylor series of the capability by settling the recursive condition from the given differential condition. Zhou [30] was quick to start the differential change strategy (DTM).

Persuaded by above examinations the current paper manages the MHD crushing progression of Silicon Dioxide-water and Silicon Dioxide-kerosene nanofluids in presence of outside applied attractive field. A likeness change is utilized to get differential condition from the overseeing conditions. The diminished differential conditions are settled by DTM as well as by RK-4 strategy with shooting method.

MATHEMATICAL FORMULATION:

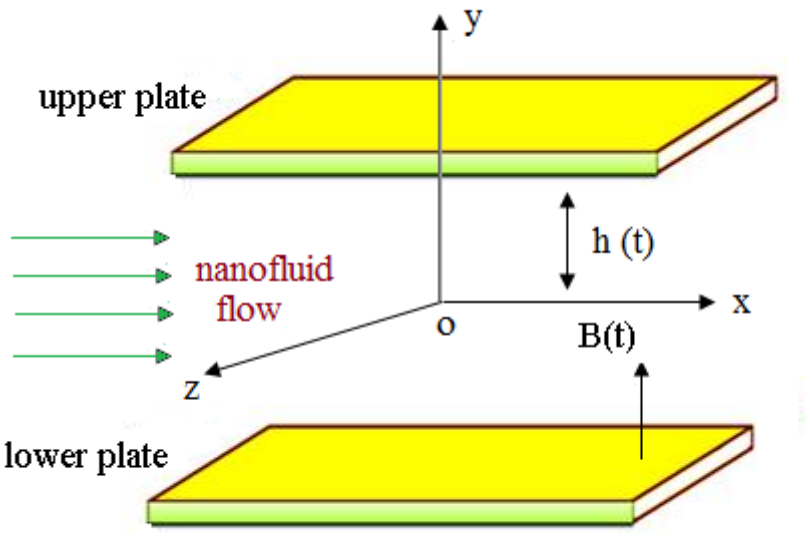

FIGURE 1: PHYSICAL MODEL OF THE PROBLEM

Consider the gooey incompressible nanofluid stream and intensity move in a two layered co-ordinate framework. The co-ordinate framework is picked in such a manner with the end goal that x-pivot is estimated along the plate and y hub is typical to the plate as displayed in the Figure 1. The pressing stream has been performed through a framework having two equal plates arranged at $h(t) = H(1-\alpha t)^{1/2}$ distance separated where $\alpha > 0$ alludes to the crushing development of the two plates with speed $v(t) = \frac{dh}{dt}$ until they contact each other at $t = \frac{1}{\alpha}$. Additionally, $\alpha < 0$ alludes to the development of the plate away to one another and is known as the trademark boundary having aspect of time reverse. H is the underlying place of the plate at time t= 0. A uniform attractive field of solidarity is applied along the typical to the plate where $B(t) = B_0(1-\alpha t)^{-1/2}$ is the underlying force of the attractive field. In the numerical definition conspire we continue with the accompanying presumption that there is no substance response, radiative intensity move, nanoparticles and base liquid are in warm balance and no slip happens between them. All body powers are thought to be dismissed. Here we have considered two kinds of nanofluids Silicon Dioxide-water and Silicon Dioxide-kerosene. The thermophysical properties of the nanofluid are given in Table 1.

TABLE 1: THERMOPHYSICAL PROPERTIES OF WATER, KEROSENE, SILICON DIOXIDE NANOPARTICLES

	ρ (Kg/m^3)	C_p (J/kg.K)	κ (W/m.K)
Pure water	997.1	4179	0.613
Kerosene	780	2090	0.149
Silicon Dioxide	2220	745	1.4

Under the above stated situation, the governing equations are as follows:

$$\frac{\partial u}{\partial x}+\frac{\partial v}{\partial y}=0 \tag{1}$$

$$\rho_{nf}\left(\frac{\partial u}{\partial t}+u\frac{\partial u}{\partial x}+v\frac{\partial u}{\partial y}\right)=-\frac{\partial p}{\partial x}+\mu_{nf}\left(\frac{\partial^2 u}{\partial x^2}+\frac{\partial^2 u}{\partial y^2}\right)-\sigma B^2(t)u \tag{2}$$

$$\rho_{nf}\left(\frac{\partial v}{\partial t}+u\frac{\partial v}{\partial x}+v\frac{\partial v}{\partial y}\right)=-\frac{\partial p}{\partial y}+\mu_{nf}\left(\frac{\partial^2 v}{\partial x^2}+\frac{\partial^2 v}{\partial y^2}\right) \tag{3}$$

$$\begin{aligned}&\frac{\partial T}{\partial t}+u\frac{\partial T}{\partial x}+v\frac{\partial T}{\partial y}=\frac{k_{nf}}{(\rho C_p)_{nf}}\left(\frac{\partial^2 T}{\partial x^2}+\frac{\partial^2 T}{\partial y^2}\right)\\&+\frac{\mu_{nf}}{(\rho C_p)_{nf}}\left[4\left(\frac{\partial u}{\partial x}\right)^2+\left(\frac{\partial u}{\partial y}+\frac{\partial v}{\partial x}\right)^2\right]+\tau\left\{D_{BM}\frac{\partial T}{\partial y}\frac{\partial C}{\partial y}+\frac{D_{TP}}{T_H}\left(\frac{\partial T}{\partial y}\right)^2\right\},\end{aligned} \tag{4}$$

$$\frac{\partial C}{\partial t}+u\frac{\partial C}{\partial x}+v\frac{\partial C}{\partial y}=D_{BM}\frac{\partial^2 C}{\partial y^2}+\frac{D_{TP}}{T_H}\frac{\partial^2 T}{\partial y^2} \tag{5}$$

where u, v are the speed parts in x and y bearings separately. Here T,C p, ρ_{nf}, μ_{nf}, $(\rho C_p)_{nf}$, k_{nf} addresses the temperature, nanofluid focus, pressure, compelling thickness, powerful unique consistency, successful intensity limit and viable warm conductivity of the nanofluids individually. Presently the relations between base liquid and nanoparticles are given by

$$\rho_{nf}=(1-\phi)\rho_f+\phi\rho_s \tag{6}$$

$$(\rho C_p)_{nf}=(1-\phi)(\rho C_p)_f+\phi(\rho C_p)_s \tag{7}$$

$$\mu_{nf}=\frac{\mu_f}{(1-\phi)^{2.5}} \tag{8}$$

$$\frac{k_{nf}}{k_f}=\frac{k_s+2k_f-2\phi(k_f-k_s)}{k_s+2k_f+\phi(k_f-k_s)} \tag{9}$$

The relevant boundary conditions for the present problem are as follows:

$$\left.\begin{aligned} &u=0,\ v=0,\ \frac{\partial T}{\partial y}=0, C=C_0 \text{ at y=0} \\ &u=0,\ v=\frac{dh}{dt},\ T=T_H, \text{C=C}_H \text{ at } y=h(t) \end{aligned}\right\} \tag{10}$$

Presently to change over the fractional differential condition into normal differential conditions, let us present the accompanying dimensionless capabilities f,θ,φ and closeness variable η as follows:

$$\left.\begin{aligned} &u=\frac{\alpha x}{2(1-\alpha t)} f'(\eta),\ \theta=\frac{T}{T_H}, \varphi=\frac{C-C_H}{C_0-C_H}\ v=\frac{-\alpha H}{\sqrt{1-\alpha t}} f(\eta), \\ &B(t)=B_0(1-\alpha t)^{-1/2},\ \ \eta=\frac{y}{H\sqrt{1-\alpha t}} \end{aligned}\right\} \tag{11}$$

where prime denotes the differentiation with respect to η.Using the above transformation and simplifying equation (2), (3) by eliminating pressure terms we have

$$f^{iv}-S.A_1(1-\phi)^{2.5}\left(3f''+\eta f'''+ff''-f.f'''\right)-M^2 f''=0 \tag{12}$$

$$\theta''+\Pr.\left(\frac{A_2}{A_3}\right)\left\{S.(f\theta'-\eta\theta')+N_{BM}\varphi'\theta'+Nt\left(\theta'\right)^2\right\}$$
$$+\frac{\Pr.Ec}{A_3(1-\phi)^{2.5}}(f''^2+4\delta^2 f'^2)=0 \tag{13}$$

$$\varphi''+\left(\frac{A_2}{A_3}\right)\left(Lef\varphi'+\frac{Nt}{Nb}\theta''\right)=0 \tag{14}$$

with associate the boundary conditions

$$\left.\begin{aligned} &f''(0)=0,\ f(0)=0, \theta'(0)=0, \varphi(0)=1 \ \text{ for } \eta=0, \\ &f'(1)=0,\ f(1)=1, \theta(1)=1, \varphi(1)=0 \quad \text{ for } \eta=1 \end{aligned}\right\} \tag{15}$$

where , $A_1=(1-\phi)+\phi\frac{\rho_s}{\rho_f}$, $A_2=(1-\phi)+\phi\frac{(\rho C_p)_s}{(\rho C_p)_f}$, $A_3=\frac{k_s+2k_f-2\phi(k_f-k_s)}{k_s+2k_f+\phi(k_f-k_s)}$, $S=\frac{\alpha H^2}{2\nu_f}$ indicates the press number having the property S>0 compares to the plates are moving separated and S<0 relates to the plates moving to one another, $\Pr=\frac{\mu_f(\rho C_p)_f}{\rho_f k_f}$ is the Prandtl number, $Ec=\frac{\rho_f}{(\rho C_p)_f T_H}\left[\frac{\alpha x}{2(1-\alpha t)}\right]^2$ is the Eckert number, $N_{BM}=\frac{\tau D_B\left(C_H-C_0\right)}{\alpha_f}$ is Brownian

movement boundary, $N_{TP} = \frac{\tau D_{TP}}{\alpha_f}$ is thermophoresis boundary, $M = \frac{\sigma_{nf}}{\mu_{nf}} H^2 \alpha {B_0}^2$ is the Hartman number, $\delta = \frac{H^2(1-\alpha t)}{x^2}$ is the dimensionless length, $Le = \frac{\alpha_f}{D_B}$ is Lewis number.

The actual amounts which have viable interest in designing are the skin erosion coefficient and Nusselt number can be characterized separately as follows:

$$C_f = \frac{\mu_{nf}\left(\frac{\partial u}{\partial y}\right)_{y=h(t)}}{\frac{1}{2}\rho_{nf}\left(\frac{dh}{dt}\right)^2}, \quad Nu = \frac{-k_{nf}\left(\frac{\partial T}{\partial y}\right)_{y=h(t)}}{kT_H} \tag{16}$$

In terms of dimensionless variables, the reduced skin friction coefficient and the reduced Nusselt number are respectively given by

$$\left.\begin{aligned} C_{fr} &= \frac{\mathrm{Re}_x C_f H^2 \sqrt{1-\alpha t}}{2x^2} = \frac{f''(1)}{A_1(1-\phi)^{2.5}}, \\ Nu_r &= Nu.\sqrt{1-\alpha t} = -A_3\theta'(1) \end{aligned}\right\} \tag{17}$$

where $\mathrm{Re}_x = \frac{x\alpha H}{2\nu_f}$ is the local Reynolds number.

TABLE 2 DIFFERENTIAL TRANSFORMATIONS OF SOME FUNCTIONS:

Original function	T-function
$h(\lambda) = \frac{d^m g(\lambda)}{d\lambda^m}$	$H[k] = \frac{(k+m)!}{k!} G[k+m]$
$h(\lambda) = g(\lambda).p(\lambda)$	$H[k] = \sum_{n=0}^{k} G[n]P[k-n]$
$h(\lambda) = \lambda^n$	$H[k] = \delta(k-n) = \begin{cases} 1, k = n \\ 0, k \neq n \end{cases}$
$h(\lambda) = \alpha g(\lambda) \pm \beta p(\lambda)$	$H[k] = \alpha G[k] \pm \beta P[k]$

SOLUTION METHODOLOGY:

We can define a function $g(\lambda)$ in differential transformation method as follows:

$$G(k) = \frac{1}{k!}\left[\frac{d^k g(\lambda)}{d\lambda^k}\right]_{\lambda=\lambda_0} \tag{18}$$

where $G(k)$ is called the T-function or simply transformed form of $g(\lambda)$. The inverse transformation of $G(k)$ is defined as

$$g(\lambda)=\sum_{k=0}^{\infty}G(k).(\lambda-\lambda_0)^k \tag{19}$$

Now putting the value of $G(k)$ in (19) as we defined earlier in (18) we can rewrite (19) as

$$g(\lambda)=\sum_{k=0}^{\infty}\frac{1}{k!}\left[\frac{d^k g(\lambda)}{d\lambda^k}\right]_{\lambda=\lambda_0}(\lambda-\lambda_0)^k \tag{20}$$

In the upcoming solution procedure profile, we have used some of the basic operations of DTM which we have listed in Table 2.

Now applying DTM in the equation (12), we can obtain

$$\left.\begin{aligned}&(k+1)(k+2)(k+3)(k+4)F\left[k+4\right]\\&-SA_1(1-\phi)^{2.5}\sum_{m=0}^{k}\left(\Delta\left[k-m-1\right](m+1)(m+2)(m+3)F\left[m+3\right]\right)\\&-3SA_1(1-\phi)^{2.5}(k+1)(k+2)F\left[k+2\right]\\&-SA_1(1-\phi)^{2.5}\sum_{m=0}^{k}\left((k-m+1)F\left[k-m+1\right](m+1)(m+2)F\left[m+2\right]\right)\\&+SA_1(1-\phi)^{2.5}\sum_{m=0}^{k}\left(F\left[k-m\right](m+1)(m+2)(m+3)F\left[m+3\right]\right)=0\end{aligned}\right\} \tag{21}$$

Where $\Delta(m)=\begin{cases}1, m=1\\0, m\neq 1\end{cases}$.

The corresponding boundary conditions are transformed as

$$F\left[0\right]=0, F\left[1\right]=k_1, F\left[2\right]=0, F\left[3\right]=k_2 \tag{22}$$

Similarly, we have from (13)

$$\left.\begin{aligned}&(k+1)(k+2)\Theta\left[k+2\right]+\Pr.S.\left(\frac{A_2}{A_3}\right)\sum_{m=0}^{k}\left(F\left[k-m\right](m+1)\Theta\left[m+1\right]\right)\\&+\Pr.\left(\frac{A_2}{A_3}\right)\sum_{m=0}^{k}\left(\begin{matrix}N_{BM}\left(k-m+1\right)\left(m+1\right)\Theta\left[k-m+1\right]\Phi\left[m+1\right]\\+\left(k-m+1\right)\left(m+1\right)\Theta\left[k-m+1\right]\Phi\left[m+1\right]\end{matrix}\right)\\&-\Pr.S.\left(\frac{A_2}{A_3}\right)\sum_{m=0}^{k}\left(\Delta\left[k-m\right](m+1)\Theta(m+1)\right)\\&+\frac{\Pr.Ec}{A_3(1-\phi)^{2.5}}\sum_{m=0}^{k}\left((k-m+1)(k-m+2)F\left[k-m+2\right](m+1)(m+2)F\left[m+2\right]\right)\\&+\frac{\Pr.Ec.4\delta^2}{A_3(1-\phi)^{2.5}}\sum_{m=0}^{k}\left((k-m+1)F\left[k-m+1\right](m+1)F\left[m+1\right]\right)=0\end{aligned}\right\} \tag{23}$$

The relevant boundary conditions become

$$\Theta[0]=k_3,\Theta[1]=0$$

(24)

Similarly, we have from (14)

$$\left.\begin{aligned}&(k+1)(k+2)\Phi[k+2]+Le\left(\frac{A_2}{A_3}\right)\sum_{m=0}^{k}\left(F[k-m](m+1)\Theta[m+1]\right)\\&+\frac{Nt}{Nb}\left(\frac{A_2}{A_3}\right)(k+1)(k+2)\Theta[k+2]=0\end{aligned}\right\}$$

(25)

The relevant boundary conditions become

$$\Theta[0]=1,\Theta[1]=0$$

(26)

where $F[k],\Theta[k],\Phi[k]$ are the transformed form of $f(\eta),\theta(\eta),\varphi(\eta)$ and k_1,k_2,k_3 are the constants which can be obtained using the boundary condition. Now the iteration scheme is as follows:

$$\left.\begin{aligned}&F[0]=0,\ F[1]=k_1,\ F[2]=0,\ F[3]=k_2,\ F[4]=0,\\&F[5]=\frac{3}{20}S.A_1(1-\phi)^{2.5}k_2+\frac{1}{20}M^2.k_2,\\&F[6]=\frac{1}{360}\left[\left(6+\frac{9.M^2}{5}\right)S.A_1(1-\phi)^{2.5}k_2+\frac{3}{5}M^4.k_2\right],.....\end{aligned}\right\}$$

(27)

$$\left.\begin{aligned}&\Theta[0]=k_3,\ \Theta[1]=0,\ \Theta[2]=-\frac{\Pr.Ec.2\delta^2k_1^2}{A_3(1-\phi)^{2.5}},\ \Theta[3]=0,\\&\Theta[4]=\Pr.S.\left(\frac{A_2}{A_3}\right)\left(\frac{1-k_1}{6}\right).\Theta[2]-\frac{\Pr.Ec}{A_3(1-\phi)^{2.5}}\left[4k_2^2+2k_1k_2\delta^2\right],\ .....\end{aligned}\right\}$$

(28)

Substituting the above equations (27), (28) into the main equation based on DTM we can obtain the following solutions:

$$\left.\begin{aligned}&f(\eta)=k_1\eta+k_2\eta^3+\left(\frac{3}{20}S.A_1(1-\phi)^{2.5}k_2+\frac{1}{20}M^2.k_2\right)\eta^5\\&+\frac{1}{360}\left[\left(6+\frac{9.M^2}{5}\right)S.A_1(1-\phi)^{2.5}k_2+\frac{3}{5}M^4.k_2\right]\eta^6+.....\end{aligned}\right\}$$

(29)

$$\theta(\eta) = k_3 - \frac{\Pr.Ec.2\delta^2 k_1^2}{A_3(1-\phi)^{2.5}}\eta^2 + \left[\begin{array}{l} \Pr.S.\left(\frac{A_2}{A_3}\right)\left(\frac{1-k_1}{6}\right).\Theta[2] \\ -\frac{\Pr.Ec}{A_3(1-\phi)^{2.5}}\left[4k_2^2 + 2k_1k_2\delta^2\right] \end{array}\right]\eta^4 + \ldots. \tag{30}$$

Considering $\eta = 1,\ S = 0.5,\ \Pr = 0.71,\ Ec = 0.5,\ M = 0.5,\ \delta = 0.1$ one can easily get $k_1 = 1.460028967,\ k_2 = -0.420057934,\ k_3 = 1.016183698$.

Now we proceed to solve numerically the equations (12) and (13) together with the boundary conditions (15) by switching them to an initial value problem. The equations (12) and (13) can be written in the form of first order differential equations as follows:

$$\left.\begin{array}{l} f' = z \\ z' = p \\ p' = q \\ q' = S.A_1.(1-\phi)^{2.5}\left(3p + \eta q + zp - fq\right) + M^2 p \end{array}\right\} \tag{31}$$

$$\left.\begin{array}{l} \theta' = r \\ r' = -\Pr.S.\frac{A_2}{A_3}.\left(fr - \eta r\right) - \frac{\Pr.Ec}{A_3.(1-\phi)^{2.5}}.\left(p^2 + 4\delta^2 z^2\right) \end{array}\right\} \tag{32}$$

Since the situations (31) and (32) are beginning worth issue, consequently to incorporate them we really want an incentive for $z(0)$ i.e., $f'(0)$, $p(0)$ i.e., $f''(0)$, $q(0)$ i.e., $f'''(0)$ and r i.e., $\theta'(0)$. We know the worth of $\theta'(0)$ and $f''(0)$ from the limit condition. Yet, no such qualities for $f'(0)$ and $f'''(0)$ are given in the limit conditions. So, we make some legitimate speculation of $f'(0)$ and $f'''(0)$. After that incorporation is done and contrast and the upsides of $f'(0)$, $f'''(0)$. We change the worth of $f'(0)$, $f'''(0)$, to acquire better estimate of the arrangement $f'(0)$, $f'''(0)$. We take the series of values for $f'(0)$, $f'''(0)$, and apply RK-4 technique with various upsides of step-sizes, for example, $h = 0.01, 0.001, \ldots.$ and so on. The inward cycle is finished with the union model of 10^{-6} in all cases.

TABLE 3 VALUES $f''(1)$ OF SILICON DIOXIDE-WATER FOR VARIOUS VALUES OF S:

S	$f''(1)$	
	DTM	RK-4
0.5	-3.413019	-3.413020
1.0	-3.736838	-3.736839
1.5	-4.030501	-4.030502
2.0	-4.030037	-4.030038

2.5	-4.551056	-4.551057

To check the productivity of RK-4, a correlation between logical arrangement got by DTM and mathematical arrangement got by RK-4 is classified in Table 3. Here we have determined the $f''(1)$ upsides of Silicon Dioxide-water for different upsides of press number S. The outcomes got are in great understanding. Then again to check the legitimacy of our current work we consider what is going on of Silicon Dioxide-water nanofluid without attractive field when two plates are moving separated i.e., S>0. We organize what is happening in numerical condition by letting the upsides of boundary as $S = 0.5, \delta = 0.1, M = 0.0, \phi = 0.0$.

TABLE 4 VALUES OF $-\theta'(1)$ FOR VARIOUS VALUES OF Pr, Ec

Pr	Ec	Mustafa et al. [10]	Pourmehran et al. [22]	Present work
0.5	1.0	1.522368	1.518859607	1.522367498
1.0	-	3.026324	3.019545607	3.026323559
2.0	-	5.98053	5.967887511	5.980530398
5.0	-	14.43941	14.41394678	14.43941324
1.0	0.5	1.513162	1.509772834	1.513161807
-	1.2	3.631588	3.623454726	3.631588269
-	2.0	6.052647	6.039091204	6.052647108
-	5.0	15.13162	15.09772808	15.13161784

TABLE 5 EFFECTS OF S ON Cf_r AND Nu_r

S	Cf_r		Nu_r	
	Silicon Dioxide-water	Silicon Dioxide-kerosene	Silicon Dioxide-water	Silicon Dioxide-kerosene
-1.0	-1.938344	-1.819084	1.225071	1.232899
0.5	-3.096871	-2.983827	1.137759	1.138204
1.0	-3.390695	-3.275727	1.119464	1.111067

We have determined the upsides of Nusselt number $-\theta'(1)$ for different upsides of Pr and Ec and arranged these qualities in Table 4. We see that the qualities are in phenomenal concurrence with Mustafa et al.[10] and Pourmehran et al.[22].

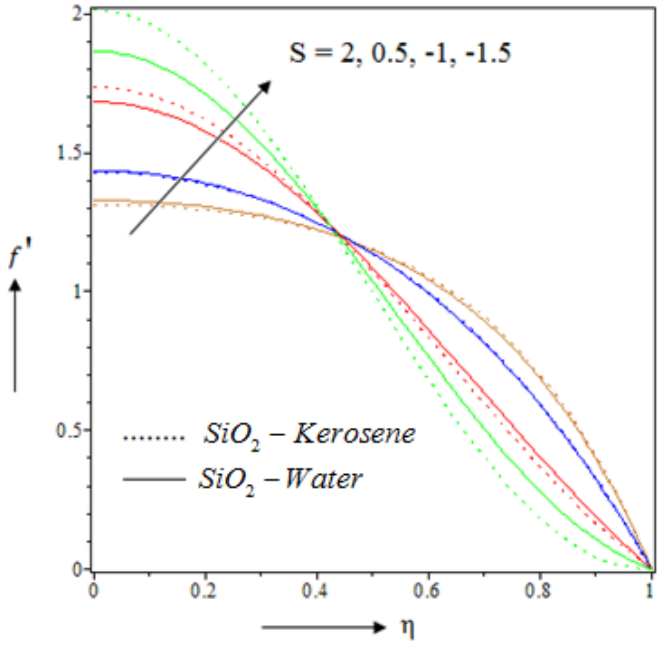

FIGURE 2: EFFECTS OF SQUEEZING PARAMETER S ON VELOCITY

RESULT AND DISCUSSION:

In this segment we will talk about the impacts of different actual boundaries on speed appropriation and temperature circulation. The entire conversation has been performed through charts and tables. In the recreation the default upsides of the boundaries are taken as $\Pr = 0.71,\ Ec = 0.5,\ M = 0.5,\ S = 0.5,\ \delta = 0.1,\ \phi = 0.15$ except if generally determined.

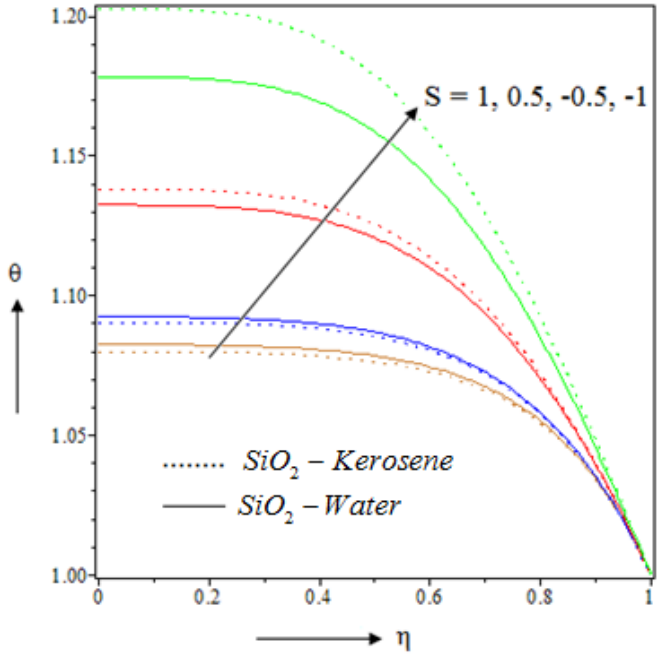

FIGURE 3: EFFECTS OF SQUEEZING PARAMETER S ON TEMPERATURE

TABLE 6: EFFECTS OF ϕ M ON Cf_r

ϕ	M	Cf_r			
		Silicon Dioxide-water		Silicon Dioxide-kerosene	
		S = 0.5	S = -0.5	S = 0.5	S = -0.5
0.02	0.5	-3.096871	-2.388320	-2.983826	-2.274793
0.04	-	-2.889905	-2.180419	-2.711130	-2.000632
0.06	-	-2.736134	-2.025792	-2.515986	-1.804083
0.02	1.5	-3.402609	-2.773329	-3.275986	-2.646386
-	3	-4.277192	-3.811202	-4.112513	-3.646416
-	4.5	-5.414585	-5.074220	-5.201616	-4.861222

EFFECT OF S ON VELOCITY AND TEMPERATURE PROFILES:

Figure 2 exhibits the impact of the pressing boundary S on nanofluid speed. It uncovers that for $0 \le \eta \le 0.42$ (not entirely set in stone) the speed profile diminishes with expanding S yet for $\eta > 0.42$ (not entirely settled) it begins expanding as displayed in the figure. Actually, this can be made sense of that the diminishing in the liquid speed close to the wall area causes to increment speed slope there. Since the mass stream rate is kept moderate consequently a lessening in the liquid speed close to the wall locale will be repaid by the rising liquid speed close to the focal district. That is the reason at $\eta = 0.42$ (not entirely settled) we found a place of division and discharge happens. Likewise, the pace of diminishing in the liquid speed for Silicon Dioxide-water is faster than Silicon Dioxide-kerosene inside the locale $0 \le \eta \le 0.42$. Be that as it may, the impact is inverse for $\eta > 0.42$. From Table 5 we see that the diminished skin erosion coefficient diminishes as S increments for both Silicon Dioxide-water and Silicon Dioxide-kerosene.

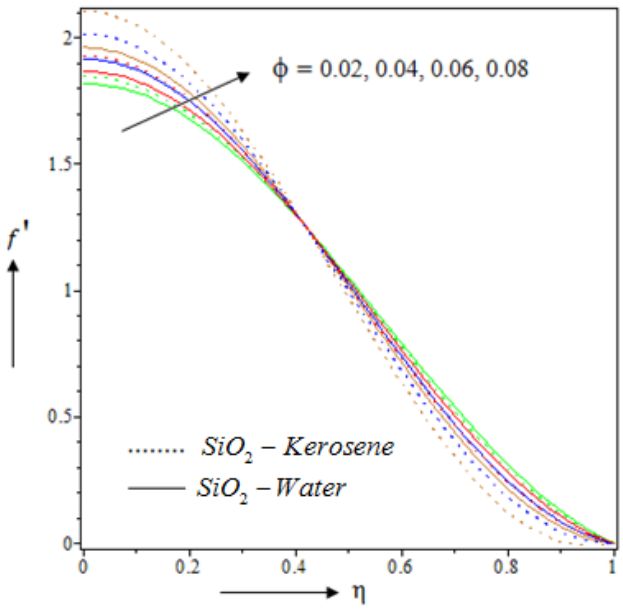

FIGURE 4: EFFECT OF NANOPARTICLE VOLUME FRACTION ON VELOCITY WHEN S<0

TABLE 7: EFFECTS OF ϕ , M, EC ON Nu_r

ϕ	M	Ec	Nu_r			
			Silicon Dioxide-water		Silicon Dioxide-kerosene	
			S = 0.5	S = -0.5	S = 0.5	S = -0.5
0.02	0.5	0.5	1.137759	1.160594	1.138203	1.162025
0.04	-	-	1.199843	1.223263	1.200806	1.226410
0.06	-	-	1.266466	1.290603	1.267997	1.295712
0.02	1.5	-	1.157179	1.149260	1.157937	1.149597
-	3.0	-	1.251637	1.206060	1.252779	1.205117
-	4.5	-	1.426942	1.376159	1.428062	1.375016
0.02	0.5	0.5	2.275519	2.321188	2.276407	2.324051
-	-	1.5	3.413278	3.481782	3.414611	3.486075
-	-	2.5	4.551038	4.642375	4.552815	4.648101

Figure 3 shows that the nanofluid temperature diminishes as S increments. Since $S = \frac{\alpha H^2}{2\nu_f}$ consequently expansion in the crushing boundary S addresses the reduction in kinematic consistency as well as the speed at which the plates move separated. Thus, grating between the limit surface of the plate and nanoparticles lessens thus the temperature of the nanofluid. This outcome is viewed as indistinguishable with Mustafa et al. [10]. Table 5 shows that Nusselt number declines with expanding S for both Silicon Dioxide-water and Silicon Dioxide-kerosene.

EFFECT OF ϕ ON VELOCITY AND TEMPERATURE PROFILES:

Figure 4 and Figure 5 portray the impact nanoparticle volume division on nanofluid speed for S>0 and S<0. It has been found that for $0 \le \eta \le 0.42$ (not set in stone) speed increments as ϕ increments yet the impact is inverse for $\eta > 0.42$ (still up in the air). The idea of the impact is same for both for S>0 and S<0. Yet, when two plates are moving separated i.e., S>0 then the speed of Silicon Dioxide-kerosene is less when contrasted with Silicon Dioxide-water inside the district $0 \le \eta \le 0.42$. Anyway the impact is inverse and unmistakable when S<0 i.e., supposed pressing stream. From Table 6 it is seen that the impact of ϕ builds the decreased skin rubbing coefficient Cf_r for both Silicon Dioxide-water and Silicon Dioxide-kerosene.

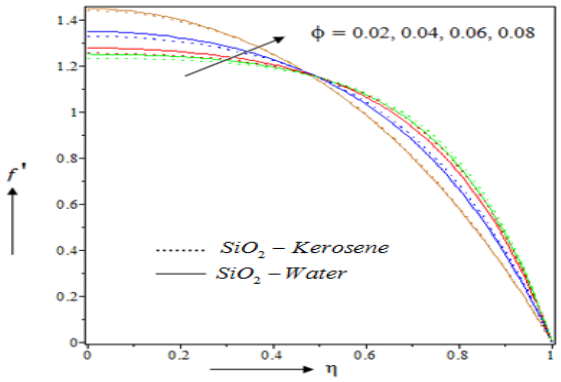

FIGURE 5: EFFECT OF NANOPARTICLE VOLUME FRACTION ON VELOCITY WHEN S>0

We have addressed the temperature profiles against η for different upsides of nanoparticle volume division in Figure 6 and Figure 7 for both S<0 and S>0 separately. Figure 6 shows that the liquid temperature has high worth due to expanding the upsides of for S<0 i.e., the pressing stream. The purpose for the peculiarities is that when two plates move to one another and nanoparticle volume expands there are more crash among nanoparticles and particles with the limit surface of the plate and subsequently the subsequent grinding leads to build the temperature inside the liquid close to the limit district. It ought to be noticed that liquid temperature of Silicon Dioxide-kerosene is altogether expanded when contrasted with Silicon Dioxide-water. Higher upsides of Prandtl number of kerosene are liable for this peculiarity. Be that as it may, the outcome is absolutely inverse for S>0 i.e., when two plates move separated. Then again Nusselt number increments with φ for both nanofluids as displayed Table 7.

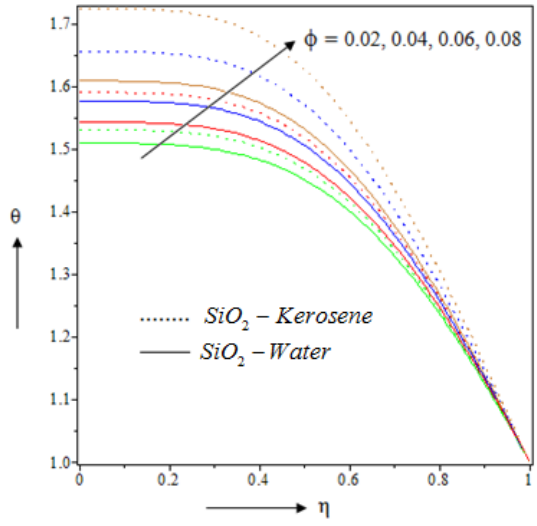

FIGURE 6: EFFECT OF NANOPARTICLE VOLUME FRACTION ON TEMPERATURE WHEN S<0

EFFECT OF M ON VELOCITY AND TEMPERATURE PROFILES:

The effect of Hartmann number M on speed dissemination are depicted in Figure 8 and Figure 9 for both S>0 and S<0. It uncovers that as M expands the speed diminishes for $0 \le \eta \le 0.42$ (not set in stone) and it is valid on the grounds that for electrically leading liquid in presence of attractive field there will continuously be Lorentz force which eases back the movement of liquid in the limit layer locale. In any case, for $\eta > 0.42$ (not entirely set in stone) the converse impact is seen due to a similar mass stream reason as examined in the past segment 4.1. Besides when S<0 two plates are exceptionally near one another, then the circumstance along with hindering Lorentz force makes antagonistic tension slope. Whenever such powers act throughout quite a while then there may be a place of division and reverse happens. For S>0 the explanation is somewhat unique. At the point when two plates move separated then an empty space happens and liquid in that locale goes with high speed so that mass stream preservation won't be disregarded.

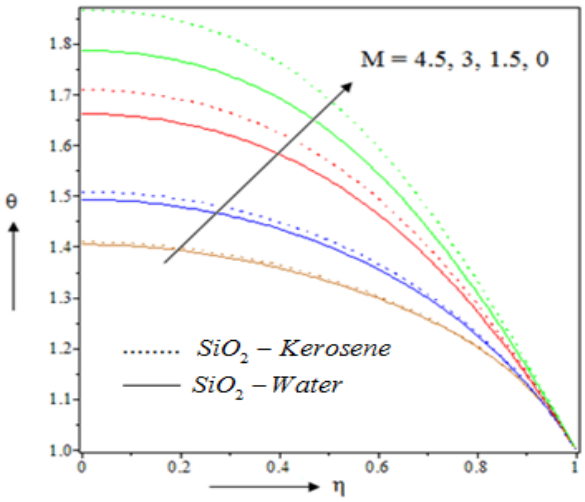

FIGURE 7: EFFECTS OF HARTMANN NUMBER M ON TEMPERATURE WHEN S<0

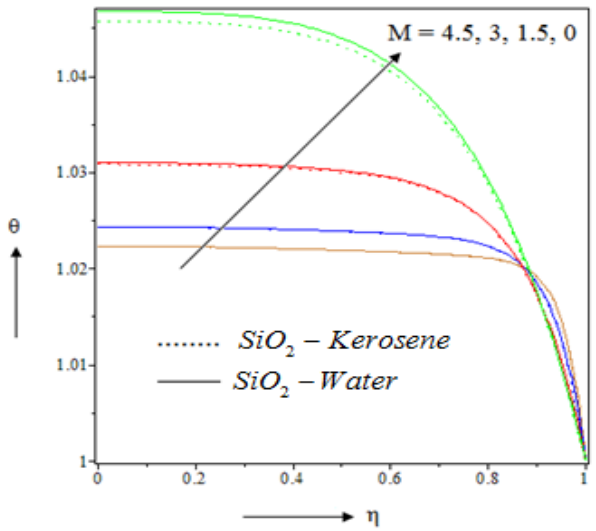

FIGURE 8: EFFECTS OF HARTMANN NUMBER M ON TEMPERATURE WHEN S>0

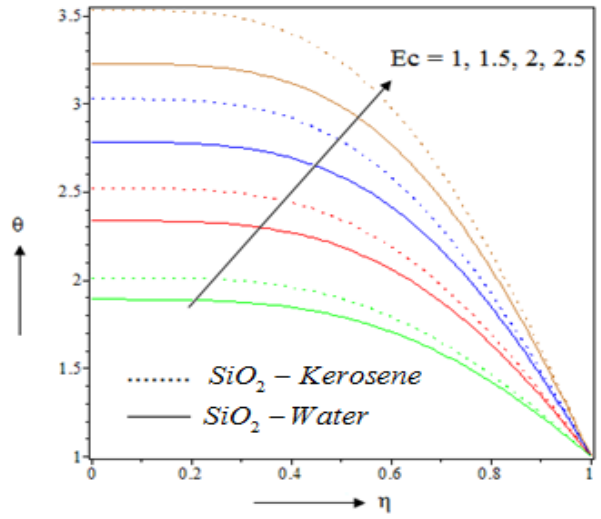

FIGURE 9: EFFECTS OF ECKERT NUMBER EC ON TEMPERATURE WHEN S<0

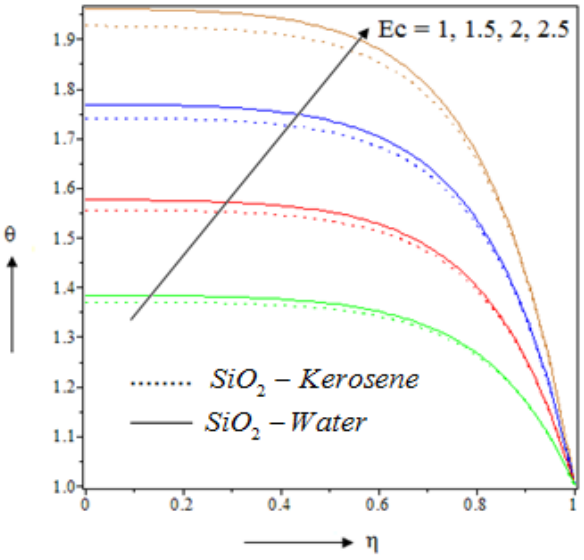

FIGURE 10: EFFECTS OF ECKERT NUMBER EC ON TEMPERATURE WHEN S>0

That is the reason for $\eta > 0.42$ we abruptly track down a sped-up stream. For $0 \le \eta \le 0.42$, speed of Silicon Dioxide-water is less when contrasted with Silicon Dioxide-kerosene for S<0 though the contrary impact happens for S>0. It ought to be noted from Table 6that diminished skin erosion coefficient Cf_r diminishes as M goes high. Figure 7-8 display that nanofluid temperature diminishes as M increments for both S<0 and S>0. For S<0 the impact is more noticeable and temperature of Silicon Dioxide-kerosene is higher than Silicon Dioxide-water nanofluid. The impact is inverse for S>0. It is worth focusing on that for S>0 we see a get over of temperature profile at η = 0.82 (still up in the air). In any case, after that district the impact is immaterial. From Table 7 we see that Nusselt number increments as M increments.

EFFECT OF ECKERT NUMBER ON TEMPERATURE PROFILES:

The impact of Eckert number Ec on nanofluid temperature profile has been depicted in Figure 12 and Figure 13 for both S>0 and S<0. It uncovers that the temperature essentially increments with the rising worth of Ec through frictional warming. Likewise, the Nusselt number increments as Ec increments for both S>0 and S<0 as displayed in Table 7. It ought to be noticed that Silicon Dioxide-kerosene have higher temperature than Silicon Dioxide-water for S<0. However, the opposite impact is seen for S>0.

CONCLUSION:

In the current paper the impact of attractive field on crushing progression of Silicon Dioxide-water and Silicon Dioxide-kerosene nanofluids has been examined. The model is changed and delivered into dimensionless structure and afterward settled scientifically utilizing differential change strategy (DTM) as well as mathematically utilizing RK-4 along with correlation with show the productivity of DTM. The mathematical conversation has been performed through diagrams and tables to delineate the subtleties of the stream qualities. In view of the entire conversation the principal finishes of our examination are as per the following:

- It is seen that liquid speed diminishes with the impact of crushing boundary and Hartmann number inside the locale $0 \le \eta \le 0.42$. Be that as it may, liquid speed increments inside a similar district due to nanoparticle volume division φ while inverse impact is seen in the two cases for $\eta > 0.42$.
- At the point when S>0 i.e., when two plates are moving separated, then the speed of Silicon Dioxide-kerosene is less when contrasted with Silicon Dioxide-water. Nonetheless, inverse impact is noticed for S<0 i.e., when two plates are moving to one another.
- Taking into account what is happening S>0 prompts decline the temperature of the liquid when nanoparticle volume division and Hartmann increment. However, the effect of Eckert number is inverse here. It is seen that the temperature of Silicon Dioxide-kerosene is less consistently when contrasted with Silicon Dioxide-water in this present circumstance. Then again, the impact is absolutely converse for S<0.
- The outcomes show an immediate connection between liquid speed and skin grating coefficient yet upgraded press number reductions the skin rubbing coefficient.
- The upgraded Hartmann number, Eckert number permit to expand Nusselt number for both Silicon Dioxide-water and Silicon Dioxide-kerosene nanofluid. In any case, it is a diminishing capability of crush number.

REFERENCES:

[1] M.J. Stefan; VersuchUberdiescheinbareadhesion; Sit- zungsberichte derAkademiederWissenschafteninWien: Mathematik-Naturwissen, 69, 713–721 (1874)

[2] Reynolds, O., 1885. On the theory of lubrication and its application to Mr. Beauchamp Tower's experiments, including an experimental determination of the viscosity of olive oil. *Phil. Trans. Roy. Soc.*, *1*, p.157.

[3] Archibald, F.R., 1956. Load capacity and time relations for squeeze films. *Transactions of the American Society of Mechanical Engineers*, *78*(1), pp.29-35.
[4] M.M Rashidi; H.Shahmohamadi; S.Dinarvand: Analytic approximate solutions for unsteady two-dimensional and axisymmetric squeezing flows between parallel plates, Math. Probl. Eng, 1-13 (2008)
[5] A.M.Siddiqui; S.Irum; A.R.Ansari: Unsteady squeezing flow of a viscous MHD fluid between parallel plates, Mathematical Modelling and Analysis, 13, 565-576 (2008)
[6] M.H.Hamdan; R.M.Baron: Analysis of the squeezing flow of dusty fluids, Appl.Sci. Res, 49, 345-354 (1992)
[7] G.Domairry; A.Aziz: Approximate analysis of MHD squeeze flow between two parallel disks with suction or injection by homotopy perturbation method, Math.Prob. Eng., 603-616 (2009)
[8] T.Hayat; A.Yousaf; M.Mustafa; S.Obaidat: MHD squeezing flow of second grad fluid between parallel disks, Int. J. Numer. Methods Fluids, 69, 399-410 (2011)
[9] M. Mahmood; S.Asghar; M.A.Hossain: Squeezed flow and heat transfer over a porous surface for viscous fluid, Heat and Mass Transfer, 44, 165-173 (2007)
[10] M.Mustafa; T.Hayat; S.Obaidat: On heat and mass transfer in the unsteady squeezing flow between parallel plates, Mechanica, 47, 1581-1589 (2012)
[11] H.M.Duwairi; B.Tashtoush; R.A.Domesh: On heat transfer effects of a viscous fluid squeezed and extruded between parallel plates, Heat and Mass Transfer, 14, 112-117 (2004)
[12] A.R.A. Khaled; K. Vafai: Hydromagnetic squeezed flow and heat transfer over a sensor surface, Int. Jour. Eng. Sci, 42, 509-519 (2004)
[13] A. Qayyum; M. Awais; A. Alsaedi; T. Hayat: Squeezing flow of non-Newtonian second grade fluids and micro-polar models, Chin. Phys. Lett, 29, 034701 (2012)
[14] A.Malvandi; D.D.Ganji: Magnetic field effect on nanoparticles migration and heat transfer of water/aluminananofluid in a channel, Jour. Magne. Mag. Materials. 362, 172–179 (2014)
[15] M.A.A.Hamad; I.Pop; Md.A.I.Ismail: Magnetic field effects on free convection flow of a nanofluid past a vertical semi-infinite flat plate, Nonlinear Analysis, Real World Applications, 12 , 1338-1346 (2011)
[16] A.Malvandi; S. A. Moshizi; D. D. Ganji: Effect of magnetic fields on heat convection inside a concentric annulus filled with Al_2O_3-water nanofluid, Advanced Powder Technology, 25, 1817-1824 (2014)
[17] A. Malvandi ; D.D. Ganji: Magnetic field and slip effects on free convection inside a vertical enclosure filled with alumina/water nanofluid, Chem. Engg. Res Design, 94, 355-364 (2015)
[18] X.Wang; X.Xu; S.U.S.Choi: Thermal conductivity of nanoparticle-fluid mixture, Jour. Thermophys.Heat Transfer, 13, 474-480 (1999)
[19] A.Mandy: Unsteady mixed convection boundary layer flow and heat transfer of nanofluids due to stretching sheet, Nuclear Engg. and Design, 249, 248-255 (2012)
[20] M. Hatami; M. Sheikholeslami; D.D.Ganji: Nanofluid flow and heat transfer in an asymmetric porous channel with expanding or contracting wall, Jour Mole Liquids, 195, 230-239 (2014)

[21] M. Hatami; M. Sheikholeslami; M. Hosseini; D.D.Ganji: Analytical investigation of MHD nanofluid flow in non-parallel walls, Jour Mole Liquids, 194, 251-259 (2014)
[22] O.Pourmehran; M.Rahimi-Gorji; M.Gorji-Bandpy; D.D.Ganji: Analytical investigation of squeezing unsteady nanofluid flow between parallel plates by LSM and CM, Alexandria Engineering Journal, 54, 17-26 (2015)
[23] M.A.Noor; S.T.Mohyud-Din; A.Waheed: Variation of parameter methodforsolving fifth-order boundaryvalue problems, AppliedMathematics and Information Sciences, 2, 135–141 (2008)
[24] S.T.Mohyud-Din;A.Yildirim: Variation of parameter method for Fishers equation, Advances in Applied Mathematics andMechanics,2, 379–388 (2010)
[25] F.Ayaz: On the two-dimensional differential transformation method, Appl. Math. Comput, 143 (2-3), 361-374 (2003)
[26] M. J. Jang; C. L. Chen; Y. C. Lin: Two-dimensional differential transformation method for solving partial differential equation, Appl. Math. Comput, 121, 261-270 (2001)
[27] M.Sheikholeslami; D.D.Ganji; H.R.Ashorynejad: Investigation of squeezing unsteady nanofluid flow using ADM, Powder Technology, 239, 259–265 (2013)
[28] S. Abbasbandy: Modified homotopy perturbation method for nonlinear equations and comparison with adomian decomposition method, Applied Mathematics and Computation,172 (1) ,431–438 (2006)
[29] R. Ellahi; M.Raza; K.Vafai: Series solutions of non-Newtonian nanofluids with Reynolds' model and Vogel's model by means of the homotopy analysis method, Mathematical andComputerModelling,55, 1876–1891 (2012)
[30] J. K.Zhou: Differential transformation and its application for electrical cirits, Huazhong University press, China (1986)